

# High-resolution photoemission spectroscopy for the layered antiferromagnetic $(\text{La}_{1-z}\text{Nd}_z)_{0.46}\text{Sr}_{0.54}\text{MnO}_3$ †

Tsunehiro Takeuchi,<sup>a\*</sup> Hiroshi Nozaki,<sup>a</sup> Kazuo Soda,<sup>a</sup> Takeshi Kondo,<sup>a</sup> Uichiro Mizutani,<sup>a</sup> Takayoshi Yokoya,<sup>b</sup> Takafumi Sato,<sup>c</sup> Takashi Takahashi,<sup>c</sup> Shik Shin,<sup>b</sup> Takayuki Muro,<sup>d</sup> Yuji Saitoh<sup>e</sup> and Yutaka Moritomo<sup>f</sup>

<sup>a</sup>Department of Crystalline Materials Science, Nagoya University, Nagoya 464-8603, Japan, <sup>b</sup>Institute for Solid State Physics, University of Tokyo, Kashiwa 277-8581, Japan, <sup>c</sup>Department of Physics, Tohoku University, Sendai 980-8578, Japan, <sup>d</sup>Japan Synchrotron Radiation Research Institute, SPring-8, Hyogo 679-5148, Japan, <sup>e</sup>Japan Atomic Energy Research Institute, SPring-8, Mikazuki, Hyogo 679-5148, Japan, and <sup>f</sup>Center for Integrated Research in Science and Engineering, Nagoya University, Nagoya 464-8603, Japan. E-mail: takeuchi@nuap.nagoya-u.ac.jp

High-resolution HeI photoemission spectroscopy (UPS), Mn  $2p$ – $3d$  resonant photoemission spectroscopy (RPES) and Mn  $2p$  X-ray absorption spectroscopy (XAS) have been performed to investigate the electronic structure and its effect on the electrical resistivity in  $(\text{La}_{1-z}\text{Nd}_z)_{0.46}\text{Sr}_{0.54}\text{MnO}_3$  ( $z = 0, 0.2, 0.6$  and  $1.0$ ). It was found that in the UPS and RPES spectra the Fermi edge persisted over the temperature range  $15 \leq T \leq 340$  K regardless of the magnetic structure or the composition of the samples. The density of states at the Fermi level [ $N(E_F)$ ] in the samples where  $0 \leq z \leq 0.6$  was increased drastically at the Curie temperature ( $T_C$ ) with decreasing temperature, but essentially kept unchanged across the Néel temperature ( $T_N$ ). A fairly large reduction at  $T_C$  and a small increase at  $T_N$  in the electrical resistivity with decreasing temperature are found to be well accounted for in terms of the temperature dependence of  $N(E_F)$ . The presence of a finite  $N(E_F)$  in the insulating  $\text{Nd}_{0.46}\text{Sr}_{0.54}\text{MnO}_3$  was also found. Thus the origin of the insulating behavior in this sample can be regarded as the Anderson localization associated with the small density of states and the chemical disorder between Nd and Sr.

**Keywords:** manganite; metal–insulator transition; colossal magnetoresistance; RPES; UPS; XAS.

## 1. Introduction

The cubic perovskite manganites are known to be characterized by the variety of peculiar electron transport properties, such as the colossal magnetoresistance (Jin *et al.*, 1994) associated with the magnetic-field-induced metal–insulator (MI) transition. Mn atoms in the perovskite structure provide not only itinerant electrons but also localized magnetic moments. The influence of the localized magnetic moments on the itinerant electrons is so strong that the electron transport properties of the perovskite manganites vary drastically depending on the variation in arrangement of the localized magnetic moments; the metallic conduction is in general observed for both the

ferromagnetic phase and so-called  $A$ -type layered antiferromagnetic phase, while insulating behaviors were reported for the paramagnetic and other antiferromagnetic phases (Tokura *et al.*, 1994; Urushibara *et al.*, 1995; Akimoto *et al.*, 1998; Moritomo *et al.*, 1998).

The ferromagnetic phase with metallic behavior transforms into the insulating phase accompanied by the magnetic phase transition with varying temperature or external magnetic field. This peculiar MI transition had been believed to be explained in terms of the double-exchange (DE) interaction (Anderson & Hasegawa, 1955; de Gennes, 1960). Recently, however, it was pointed out that the DE interaction alone cannot fully account for the phase transition between the ferromagnetic metal and the paramagnetic insulator (Millis *et al.*, 1995, 1996; Saitoh *et al.*, 2000). In the framework of the DE theory, the relation between the metallic conductivity and the magnetic ordering is explained as follows. The hopping probability of the itinerant electrons from one site to another is formulated by  $t = t_0 \cos(\theta/2)$ , where  $t_0$  and  $\theta$  indicate the bare hopping probability and the angle between two localized magnetic moments in the nearest-neighbor atomic sites, respectively. If these localized magnetic moments are ferromagnetically ordered, the hopping probability shows the maximum value with  $\theta = 0^\circ$ , while it is fairly reduced in the array of disordered magnetic moments and reaches zero in the array of antiferromagnetically ordered magnetic moments with  $\theta = 180^\circ$ . The reduced hopping probability leads to a reduction in the Fermi velocity. However, no increase in the electrical resistivity can be caused by it as long as a single band is concerned, because a simultaneously introduced increase in the density of states near  $E_F$  compensates the increase of the resistivity due to the reduced Fermi velocity. Thus, within the DE model, the resistivity variation cannot appear except when the phase transition between the antiferromagnetic phase and other phases occurs.

The  $A$ -type layered antiferromagnetic phase has an ordered magnetic structure in which localized magnetic moments are ferromagnetically ordered in planes and those planes stack together antiferromagnetically. Akimoto *et al.* (1998) reported the temperature dependence of the electrical resistivity for  $\text{La}_{0.46}\text{Sr}_{0.54}\text{MnO}_3$ , that possesses the paramagnetic phase above  $T_C = 300$  K, the ferromagnetic phase at  $T_N \leq T \leq T_C$  and the  $A$ -type antiferromagnetic phase below  $T_N = 200$  K. Here,  $T_C$  and  $T_N$  indicate the Curie and Néel temperatures, respectively. In their report the electrical resistivity of this sample was decreased by about 40–50% of its magnitude at  $T_C$  and slightly increased at  $T_N$  with decreasing temperature. Obviously, these behaviors cannot be understood in terms of the DE interaction. Thus in order to investigate the factors causing these behaviors in the electrical resistivity, the determination of the electronic structure of the paramagnetic state, the ferromagnetic state and the  $A$ -type antiferromagnetic state is strongly required. It should be noted here that although many experiments with photoemission spectroscopy have already been reported for the ferromagnetic and paramagnetic phases (Saitoh *et al.*, 1995, 1997; Park *et al.*, 1996; Sarma *et al.*, 1996; Chainani *et al.*, 1993, 1997; Sekiyama *et al.*, 1999), that for the  $A$ -type antiferromagnetic phase has so far not been reported.

In this paper we report the results of high-energy-resolution photoemission spectroscopy measurements for the  $(\text{La}_{1-z}\text{Nd}_z)_{0.46}\text{Sr}_{0.54}\text{MnO}_3$  ( $z = 0.0, 0.2, 0.6$  and  $1.0$ ) cubic perovskite manganites. These samples, except for  $z = 1.0$ , possess two different magnetic transitions with varying temperature; the paramagnetic phase exists above  $T_C = 230$ – $300$  K, the ferromagnetic phase at  $T_N \leq T \leq T_C$  and the  $A$ -type antiferromagnetic phase below  $T_N = 200$ – $230$  K (Akimoto *et al.*, 1998). Only  $\text{Nd}_{0.46}\text{Sr}_{0.54}\text{MnO}_3$  possesses a direct transition from the paramagnetic phase into the  $A$ -type antiferromagnetic phase at  $T_N = 225$  K without being in the ferromag-

† Presented at the ‘International Workshop on High-Resolution Photoemission Spectroscopy of Correlated Electron Systems’ held at Osaka, Japan, in January 2002.

netic phase. The electronic structure of the *A*-type antiferromagnetic phase was investigated in comparison with that of the paramagnetic and ferromagnetic phases. The relation between the measured density of states at the Fermi level [ $N(E_F)$ ] and the electrical resistivity in each compound will be discussed in detail.

## 2. Experimental

High-quality  $(La_{1-z}Nd_z)_{0.46}Sr_{0.54}MnO_3$  ( $z = 0.0, 0.2, 0.6$  and  $1.0$ ) single crystals were grown by the floating-zone method. Details of the sample preparation have been reported elsewhere (Akimoto *et al.*, 1998; Moritomo *et al.*, 1998). The bulk-sensitive Mn  $2p$ - $3d$  resonant photoemission spectroscopy (RPES) measurements (Sekiyama *et al.*, 2000) with incident photon energies of  $h\nu = 639$ – $641$  eV were performed at beamline BL25SU at the third-generation 8 GeV synchrotron radiation facility SPring-8, Hyogo, Japan. The energy resolution of the measurements was about 80–120 meV, which was determined as the energy width of the intensity drop from 90% to 10% at the Fermi edge of the reference gold electrically contacting with the samples. The HeI photoemission spectroscopy (UPS) measurements with an energy resolution of 50 meV were also performed for  $(La_{1-z}Nd_z)_{0.46}Sr_{0.54}MnO_3$  ( $z = 0.0, 0.2, 0.6$  and  $1.0$ ). All UPS and RPES measurements were carried out at temperatures between 15 K and 340 K. The sample surfaces were scraped with a diamond file just before the data accumulation at each temperature under a base pressure better than 10–11 torr. We intentionally finished each measurement within 60 min after the surface scraping to avoid the serious surface degradation reported by Saitoh *et al.* (1997). Mn  $2p$  soft X-ray absorption spectroscopy (XAS) measurements were performed at BL19B at the Photon Factory, KEK, Japan. We used a bulk-sensitive ( $\sim 2000$  Å in depth) fluorescence yield method for the present Mn  $2p$  XAS measurement.

## 3. Results and discussions

The electronic structure of these cubic perovskite manganites has been frequently studied by means of photoemission spectroscopy measurements (Saitoh *et al.*, 1995, 1997; Park *et al.*, 1996; Sarma *et al.*, 1996; Chainani *et al.*, 1993, 1997; Sekiyama *et al.*, 1999). The density of states near  $E_F$  in these reports was fairly small. Sometimes it was reported to be finite in the ferromagnetic metallic phases and to become essentially zero in the insulating phases. The small intensity near  $E_F$  prevented us from evaluating the gap width and the density of states at  $E_F$ . In order to overcome this difficulty, we employed bulk-sensitive and high-energy-resolution Mn  $2p$ - $3d$  RPES measurements, by which the density of states associated with the Mn  $3d$  electron is so enhanced that the Fermi edges are expected to be clearly observed in the metallic states.

Fig. 1(a) shows photoemission spectra of  $La_{0.46}Sr_{0.54}MnO_3$  taken with incident photon energies across the Mn  $2p$  absorption edge. All spectra are normalized by the photon flux. It can be confirmed that the intensity of the valence-band spectra increases by more than ten times when the Mn  $2p$ - $3d$  resonance takes place. The enhanced intensity due to the Mn  $2p$ - $3d$  resonance allowed us to easily observe the density of states near  $E_F$ . We employed  $h\nu = 640$  eV as the incident photon energy for the RPES measurements to avoid the effect of the undesirable auger process. Even with this incident energy the spectrum intensity is enhanced by more than five times than that of the off-resonant spectrum measured with  $h\nu = 637$  eV. The high-resolution Mn  $2p$  RPES spectra near  $E_F$  for  $(La_{0.8}Nd_{0.2})_{0.46}Sr_{0.54}MnO_3$  in the paramagnetic phase at 300 K, the ferromagnetic phase at 250 K and the *A*-type layered antiferromagnetic phase at

150 K are shown in Fig. 1(b). The clearly observed intensity at  $E_F$  in all spectra indicates that  $(La_{0.8}Nd_{0.2})_{0.46}Sr_{0.54}MnO_3$  must be metallic regardless of the magnetic status involved. It should be noted that the spectrum intensity at  $E_F$  of the ferromagnetic phase and the *A*-type antiferromagnetic phase obviously shows a much higher value than in the paramagnetic phase. The electrical resistivity of  $(La_{1-z}Nd_z)_{0.46}Sr_{0.54}MnO_3$  ( $0.0 \leq z \leq 0.4$ ) reported by Akimoto *et al.* (1998) decreases by about 50% in its magnitude when the paramagnetic phase transforms into the ferromagnetic phase at  $T_C$  but it is almost kept constant across  $T_N$ . This variation in the electrical resistivity must be caused by the variation in  $N(E_F)$  observed in the present RPES measurement.

In order to gain further insight into the electronic structure near  $E_F$  we employed the HeI UPS measurement with a higher energy resolution of 50 meV. The observed spectra for

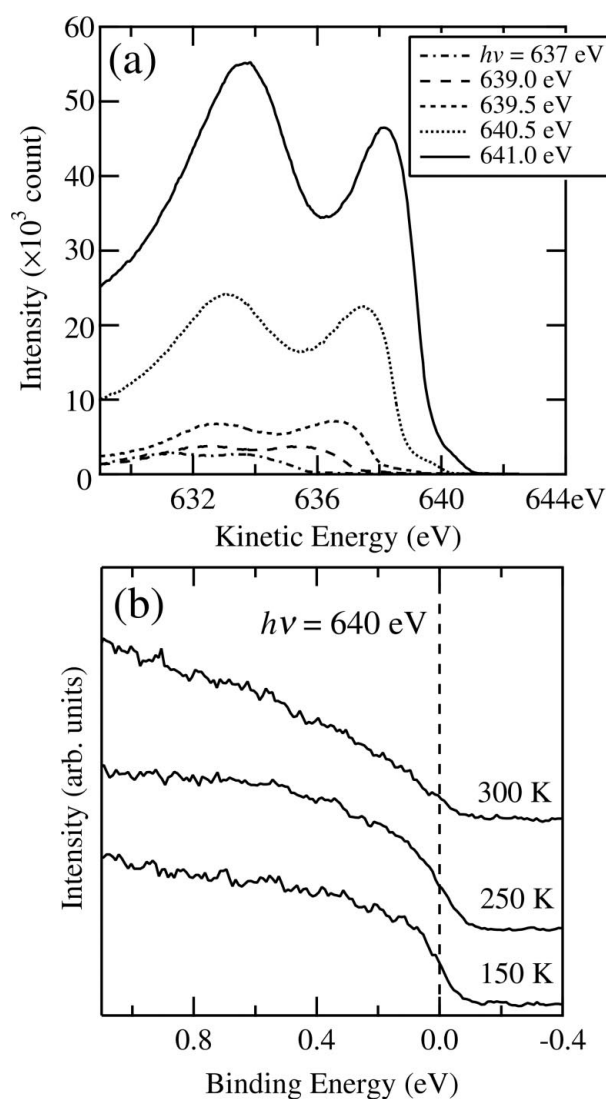


**Figure 1**  
(a) Photoemission spectra taken with incident photon energies across the Mn  $2p$  absorption edge. Mn  $2p$ - $3d$  resonance taking place at  $h\nu \geq 639$  eV allows us to clearly observe the intensity near  $E_F$ . (b) Mn  $2p$ - $3d$  RPES spectra of  $(La_{0.8}Nd_{0.2})_{0.46}Sr_{0.54}MnO_3$  perovskite manganite in the paramagnetic state at 300 K, the ferromagnetic state at 250 K and the *A*-type layered antiferromagnetic phase at 150 K measured with  $h\nu = 640$  eV. The vertical dashed line indicates the Fermi level ( $E_F$ ) determined by the reference gold. The density of states at  $E_F$  is finite in all the spectra.

$(\text{La}_{1-z}\text{Nd}_z)_{0.46}\text{Sr}_{0.54}\text{MnO}_3$  ( $z = 0.0, 0.2, 0.6$  and  $1.0$ ) at different temperatures are shown in Figs. 2(a)–2(d). Notably, all UPS spectra possess a steep Fermi edge, which shows much clearer structure than that reported for the ferromagnetic phase in the cubic perovskite manganite (Sarma *et al.*, 1996, 1997; Sekiyama *et al.*, 1999). The easiness in observing the Fermi edge with UPS measurements for the present samples most likely originates from the large O 2*p* component along with Mn 3*d* in the valence band near  $E_F$ .

The UPS spectra of  $(\text{La}_{1-z}\text{Nd}_z)_{0.46}\text{Sr}_{0.54}\text{MnO}_3$  with  $z = 0.0, 0.2$  and  $0.6$  possess a fairly large enhancement in intensity near  $E_F$  at  $T_C$  and less obvious variation across  $T_N$  with decreasing temperature. The same tendency has already been mentioned above in the RPES measurements for  $z = 0.2$ . Therefore it is certain that  $N(E_F)$  associated with both the Mn 3*d* and O 2*p* electrons increases when the phase transition from the paramagnetic phase to the ferromagnetic phase takes place, and that this variation in  $N(E_F)$  leads to the reduction in the magnitude of the electrical resistivity.

When the electrical resistivity of metallic phases is discussed in terms of the Boltzmann transport equation, we should consider not only the electronic structure but also the scattering event, that is closely related to the ordering of the local magnetic moments. It is very important to know that a reduction in the electrical resistivity of about 10% in its magnitude occurs at  $T_N$  with decreasing temperature for  $\text{Nd}_{0.46}\text{Sr}_{0.54}\text{MnO}_3$  while its UPS spectrum was almost kept unchanged across  $T_N$ . The reduction in the electrical resistivity with almost constant  $N(E_F)$  must be attributed to a reduction in the scattering probability due to the ordering of the local magnetic moments. Thus we conclude that the resistivity drop at  $T_C$  for the  $(\text{La}_{1-z}\text{Nd}_z)_{0.46}\text{Sr}_{0.54}\text{MnO}_3$  is introduced by the enhanced  $N(E_F)$  and the reduced scattering event, which cause reduction in the electrical resistivity of about 40–50% and less than 10% in its magnitude.

The electrical resistivity of  $\text{Nd}_{0.46}\text{Sr}_{0.54}\text{MnO}_3$  was reported to diverge at low temperature (Akimoto *et al.*, 1998). In sharp contrast with the divergence of the electrical resistivity, the UPS spectrum of this sample shows a clear Fermi edge at 15 K. Thus we can safely assign the insulating behavior in this sample to being caused by the Anderson localization, which is brought about by the small density of states coupled with the disorders introduced by the mixture of Nd and Sr. The other samples with  $z \leq 0.6$  do not show the Anderson localization, most likely because the relatively large density of states below  $T_C$  weakens the localization tendency of the conduction electrons.

The increase of the density of states in the vicinity of  $E_F$  for the samples with  $z \leq 0.6$  and its absence for  $z = 1.0$  were also confirmed in the conduction-band structure. The Mn 2*p* XAS spectra of  $(\text{La}_{1-z}\text{Nd}_z)_{0.46}\text{Sr}_{0.54}\text{MnO}_3$  with  $z = 0.0$  and  $1.0$  measured at room temperature and liquid-nitrogen temperature are shown in Fig. 3. A significant enhancement in  $N(E_F)$  with decreasing temperature could be observed only for  $\text{La}_{0.46}\text{Sr}_{0.54}\text{MnO}_3$ , while the intensity at  $E_F$  in  $\text{Nd}_{0.46}\text{Sr}_{0.54}\text{MnO}_3$  was kept almost unchanged. These behaviors are consistent with the present RPES and UPS spectra. Unfortunately, since we were not able to control the temperature in the XAS measurement, the exact temperature where the significant enhancement in intensity at  $E_F$  occurs was unable to be determined. However, we believe that it took place at  $T_C$  with decreasing temperature.

Let us now introduce the electronic structure commonly adopted for the cubic perovskite manganites to understand the origin of the variation in the density of states. A simple cluster-level configuration suggests that the valence band is composed of the bonding  $t2g$ , the antibonding  $t2g$ , the non-bonding O 2*p*, the bonding  $eg$  and the antibonding  $eg$  bands. Band structures calculated by LSDA and LSDA+U methods (Pickett & Singh, 1996; Madvedeva *et al.*, 2001)

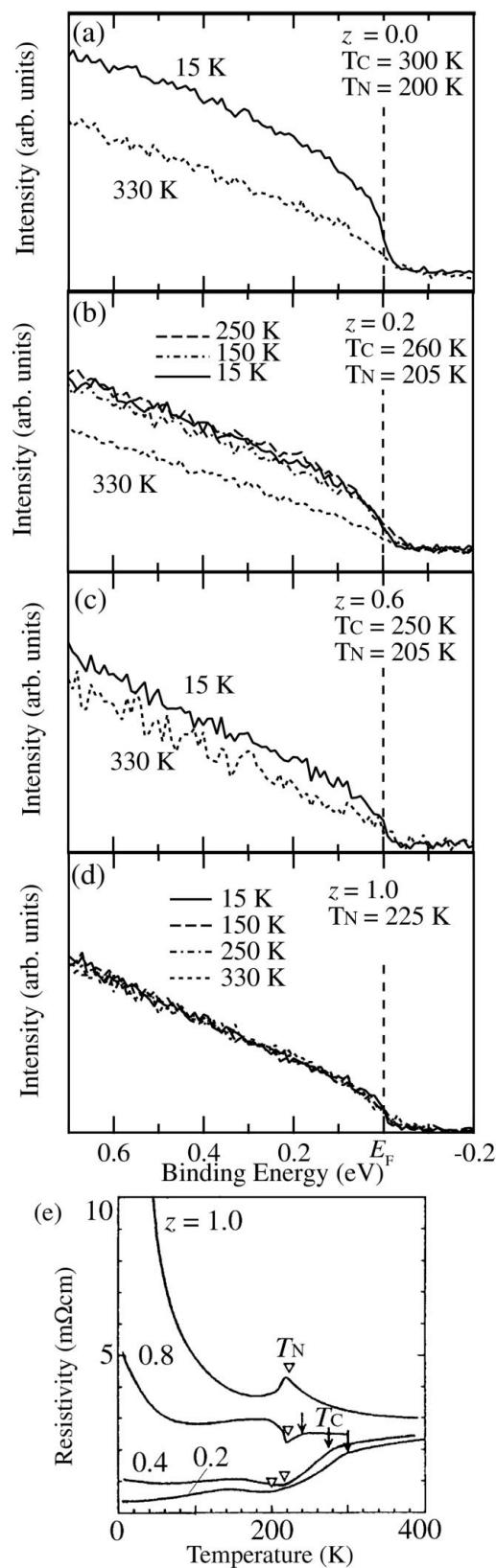


**Figure 2**

Temperature dependence of the high-resolution HeI UPS spectra near the Fermi level for  $(\text{La}_{1-z}\text{Nd}_z)_{0.46}\text{Sr}_{0.54}\text{MnO}_3$  for (a)  $z = 0$ , (b)  $z = 0.2$ , (c)  $z = 0.6$  and (d)  $z = 1.0$ . The density of states at  $E_F$  is finite in all the spectra. The vertical dashed line indicates  $E_F$  determined by the reference gold. The electrical resistivity of  $(\text{La}_{1-z}\text{Nd}_z)_{0.46}\text{Sr}_{0.54}\text{MnO}_3$  ( $z = 0.2, 0.4, 0.8$  and  $1.0$ ) reported by Akimoto *et al.* (1998) is shown in (e).

seem roughly consistent with this configuration. The bonding and antibonding bands are constructed as a consequence of the hybridization between Mn 3d and O 2p electrons. The resulting electronic structure is schematically drawn in Fig. 4. Note here that each band can involve only one electron per unit structure rather than two because of the strong on-site Coulomb interaction  $U$  and/or the on-site exchange interaction  $J$ , which were reported typically to be 4–8 eV and 0.6–0.9 eV, respectively (Madvedeva *et al.*, 2001; Mizokawa & Fujimori, 1995).

We observed a large change in the electronic structure near  $E_F$  across  $T_C$  for the samples with  $z \leq 0.6$ . This strongly indicates that a fairly large variation takes place in the antibonding  $eg$  band. If this modification in the antibonding  $eg$  band is brought about by the structure distortion about the  $\text{MnO}_6$  octahedron, the corresponding bonding  $eg$  band should also be greatly modified at the same temperature. This is in sharp contrast to the case under the influence

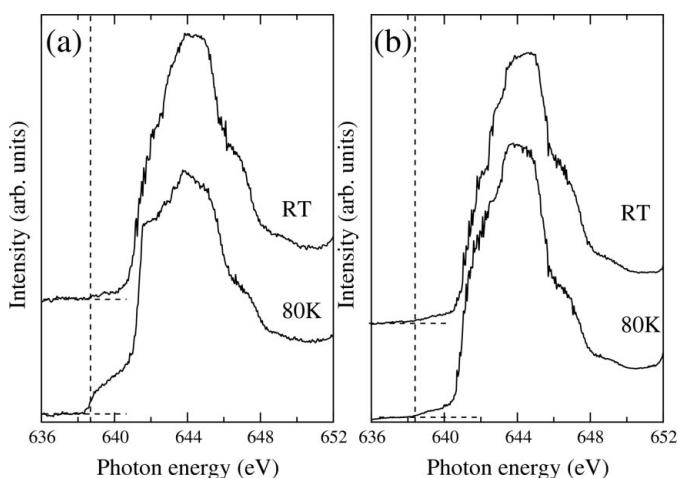


**Figure 3** Mn 2p X-ray absorption spectra for (a)  $\text{La}_{0.46}\text{Sr}_{0.54}\text{MnO}_3$  and (b)  $\text{Nd}_{0.46}\text{Sr}_{0.54}\text{MnO}_3$ . The vertical dashed line indicates the absorption edge, which corresponds to  $E_F$  in metallic samples. A large increase in the intensity just above  $E_F$  with decreasing temperature was observed only for  $\text{La}_{0.46}\text{Sr}_{0.54}\text{MnO}_3$ .

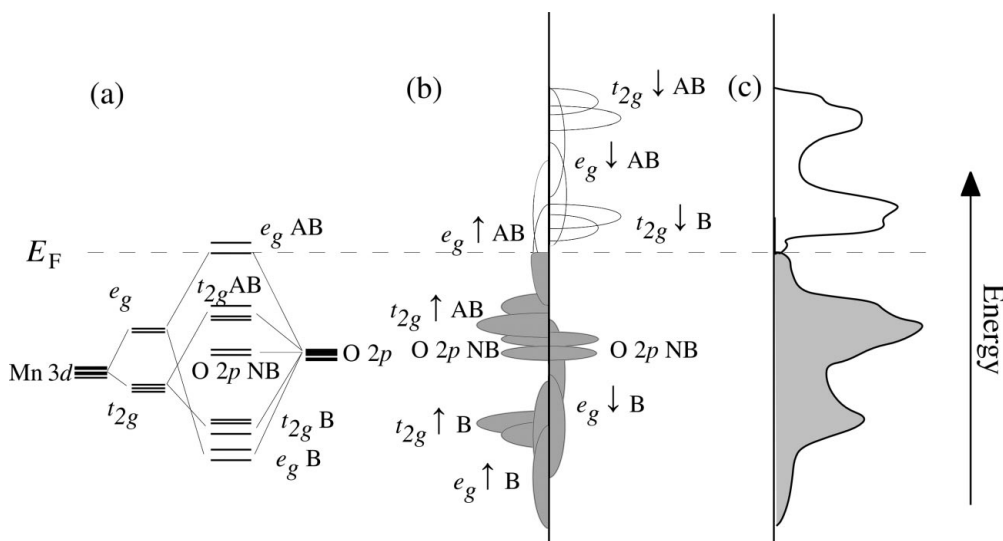


**Figure 4** Schematic drawing of (a) the cluster level, (b) the band structure and (c) the density of states expected for the cubic perovskite manganites. AB, NB and B mean anti-bonding, non-bonding and bonding levels, respectively.

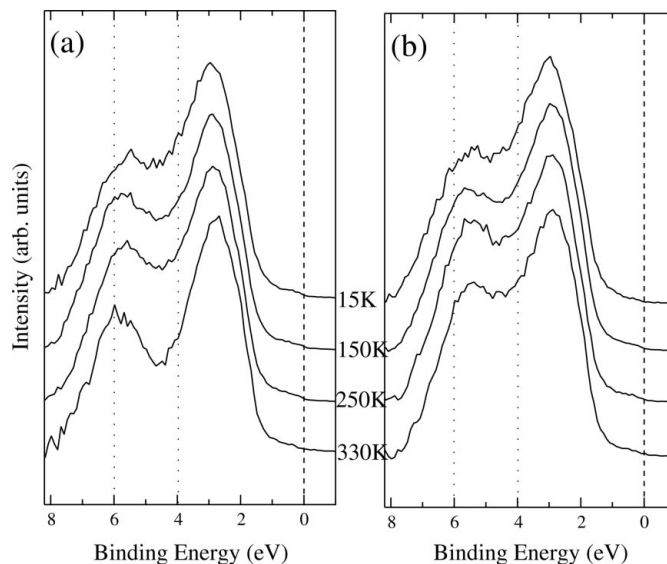


**Figure 5** Temperature dependence of the HeI UPS valence band spectra for (a)  $(\text{La}_{0.8}\text{Nd}_{0.2})_{0.46}\text{Sr}_{0.54}\text{MnO}_3$  and (b)  $\text{Nd}_{0.46}\text{Sr}_{0.54}\text{MnO}_3$ . The backgrounds were subtracted by using the Shirley method, and the spectra were normalized by the maximum intensity. A large change in the shape of the spectrum at about 4–6 eV, which is indicated as the energy-range between the dotted lines, occurred across  $T_C = 260$  K only for  $(\text{La}_{0.8}\text{Nd}_{0.2})_{0.46}\text{Sr}_{0.54}\text{MnO}_3$ .

of the DE interaction limited only upon the antibonding  $eg$  band. Thus we measured valence-band spectra for these compounds and investigated the variation in the valence-band structure below and above  $T_C$ . The temperature dependence of the UPS valence-band spectra for  $(\text{La}_{1-z}\text{Nd}_z)_{0.46}\text{Sr}_{0.54}\text{MnO}_3$  samples with  $z = 0.2$  and  $1.0$  are shown in Fig. 5. Indeed, a large modification in the valence-band structure of the sample with  $z = 0.2$  occurred at  $T_C$  in the energy range 4–6 eV where the bonding  $eg$  band most likely exists. Thus we conclude that the structure distortion occurs in the  $(\text{La}_{1-z}\text{Nd}_z)_{0.46}\text{Sr}_{0.54}\text{MnO}_3$  samples with  $0.0 \leq z \leq 0.6$  at  $T_C$  with decreasing temperature, and that it is responsible for the large enhancement in  $N(E_F)$  resulting in the reduction of the electrical

resistivity. In sharp contrast to the large change in the spectral shape of the sample with  $z = 0.2$  at 4–6 eV, the spectrum shape of the sample with  $z = 1.0$  showed less significant temperature dependence. This result agrees well with the relatively small variation in the shape of the antibonding  $eg$  band near  $E_F$  for this sample, as shown in Figs. 2(d) and 3(b). Therefore the structure distortion in the sample of  $z = 1.0$  is expected to be much smaller than that in the samples with  $z \leq 0.6$ .

Two possible structure distortions, that can lead to a variation in their electronic structure, are known to exist for the perovskite manganites. The first one is the Jahn–Teller-type (JT-type) distortion brought about inside the  $\text{MnO}_6$  octahedron. When the

degree of the JT-type distortion changes, a complicated modification would be introduced in the valence-band structure, because both the relative energy of the bands and the ratio of Mn 3d components to O 2p components in each band are drastically changed with it. The second is the GdFeO<sub>3</sub>-type distortion that contributes to the change in the one-electron bandwidth with altering Mn—O—Mn angle of the neighboring MnO<sub>6</sub> octahedra. These two structure distortions cooperatively or competitively contribute to the variation in the electronic structure at  $T_C$ . We speculate that the JT-type distortion rather than the GdFeO<sub>3</sub>-type distortion dominantly affects the electron transport properties of the present samples because the significant changes in the whole electronic structure were observed in the photoemission spectra with varying temperature.

The structure parameters of Nd<sub>0.45</sub>Sr<sub>0.55</sub>MnO<sub>3</sub> below and above  $T_N$  have already been reported (Kawano *et al.*, 1997), but the structure analysis on (La<sub>1-z</sub>Nd<sub>z</sub>)<sub>0.46</sub>Sr<sub>0.54</sub>MnO<sub>3</sub> with  $0.0 \leq z \leq 0.6$  has not been reported. Once those data are obtained, the relation between the electronic structure and the atomic structure in the cubic perovskite manganites can be quantitatively and systematically discussed. These discussions will lead to a better understanding of the electron transport behavior in these perovskite manganites.

#### 4. Conclusion

High-resolution HeI UPS, Mn 2p-3d RPES and Mn 2p XAS measurements have been performed for (La<sub>1-z</sub>Nd<sub>z</sub>)<sub>0.46</sub>Sr<sub>0.54</sub>MnO<sub>3</sub> ( $z = 0.0, 0.2, 0.6$  and  $1.0$ ), which possess phase transitions from the paramagnetic phase through the ferromagnetic phase into the A-type antiferromagnetic phase with decreasing temperature. Temperature dependence of the electrical resistivity is discussed in terms of the observed photoemission spectra. We found that the Fermi edge in (La<sub>1-z</sub>Nd<sub>z</sub>)<sub>0.46</sub>Sr<sub>0.54</sub>MnO<sub>3</sub> ( $0.0 \leq z \leq 1.0$ ) persisted over the temperature range  $15 \leq T \leq 340$  K. The temperature dependence of the electrical resistivity of these compounds was well accounted for by considering the combined effect of the varying density of states and scattering events associated with the ordering in the local magnetic moments. The former effect, which is related to the structure distortion, leads to about 50% variation at the maximum in the electrical resistivity. The latter is so weak that only less than 10% variation in the resistivity can be induced by it. The insulating behavior in Nd<sub>0.46</sub>Sr<sub>0.54</sub>MnO<sub>3</sub> at low temperature is attributed to the

Anderson localization, most likely caused by the small density of states at  $E_F$  coupled with the chemical disorder between Nd and Sr.

#### References

- Akimoto, T., Maruyama, Y., Moritomo, Y., Nakamura, A., Hirota, K., Ohoyama, K. & Ohashi, M. (1998). *Phys. Rev. B*, **57**, R5594–R5597.
- Anderson, P. W. & Hasegawa, H. (1955). *Phys. Rev.* **100**, 675–681.
- Chainani, A., Kumigashira, H., Takahashi, T., Tomioka, Y., Kuwahara, H. & Tokura, Y. (1997). *Phys. Rev. B*, **56**, R15513–R15516.
- Chainani, A., Mathew, M. & Sarma, D. D. (1993). *Phys. Rev. B*, **47**, 15397–15403.
- Gennes, P.-G. de (1960). *Phys. Rev.* **118**, 141–154.
- Jin, S., Tiefel, T. H., McCormack, M., Fasnacht, R., Ramesh, R. & Chen, L. H. (1994). *Science*, **264**, 13–16.
- Kawano, H., Kajimoto, R., Yoshizawa, H., Tomioka, Y., Kuwahara, H. & Tokura, Y. (1997). *Phys. Rev. Lett.* **78**, 4253–4256.
- Madvedeva, J. E., Anisimov, V. I., Mryasov, O. N. & Freeman, A. J. (2001). *J. Phys. Condens. Matter*, **14**, 4533–4542.
- Millis, A., Shraiman, B. I. & Mueller, R. (1996). *Phys. Rev. Lett.* **77**, 175–178.
- Millis, A. J., Littlewood, P. B. & Shraiman, B. I. (1995). *Phys. Rev. Lett.* **74**, 5144–5147.
- Mizokawa, T. & Fujimori, A. (1995). *Phys. Rev. B*, **51**, 12880–12883.
- Moritomo, Y., Akimoto, T., Nakamura, A., Ohoyama, K. & Ohashi, M. (1998). *Phys. Rev. B*, **58**, 5544–5549.
- Park, J.-H., Chen, C. T., Cheong, S.-W., Bao, W., Meigs, G., Chakarian, V. & Idzerda, Y. U. (1996). *Phys. Rev. Lett.* **76**, 4215–4218.
- Pickett, W. E. & Singh, D. J. (1996). *Phys. Rev. B*, **53**, 1146–1160.
- Saitoh, T., Bocquet, A. E., Mizokawa, T., Namatame, H., Fujimori, A., Abbate, M., Takeda, Y. & Takano, M. (1995). *Phys. Rev. B*, **51**, 13942–13951.
- Saitoh, T., Dessau, D. S., Moritomo, Y., Kimura, T., Tokura, Y. & Hamada, N. (2000). *Phys. Rev. B*, **62**, 1039–1043.
- Saitoh, T., Sekiyama, A., Kobayashi, K., Mizokawa, T., Fujimori, A., Sarma, D. D., Takeda, Y. & Takano, M. (1997). *Phys. Rev. B*, **56**, 8836–8840.
- Sarma, D. D., Shanthi, N., Krishnakumar, S. R., Saitoh, T., Mizokawa, T., Sekiyama, A., Kobayashi, K., Fujimori, A., Weschke, E., Meier, R., Kaindl, G., Takeda, Y. & Takano, M. (1996). *Phys. Rev. B*, **53**, 6873–6876.
- Sekiyama, A., Iwasaki, T., Matsuda, K., Saitoh, Y., Onuki, Y. & Suga, S. (2000). *Nature (London)*, **403**, 396–398.
- Sekiyama, A., Suga, S., Fujikawa, M., Imada, S., Iwasaki, T., Matsuda, K., Kaznacheev, K. V., Fujimori, A., Kuwahara, H. & Tokura, Y. (1999). *Phys. Rev. B*, **59**, 15528–15532.
- Tokura, Y., Urushibara, A., Moritomo, Y., Arima, T., Asamitsu, A., Kido, G. & Furukawa, N. (1994). *J. Phys. Soc. Jpn.* **63**, 3931–3935.
- Urushibara, A., Moritomo, Y., Arima, T., Asamitsu, A., Kido, G. & Tokura, Y. (1995). *Phys. Rev. B*, **51**, 14103–14109.